Article

Atmospheric Pressure Plasma-Treated Carbon Nanowalls' Surface-Assisted Laser Desorption/Ionization Time-of-Flight Mass Spectrometry (CNW-SALDI-MS)

Takayuki Ohta [1] **, Hironori Ito** [1] **, Kenji Ishikawa** [2,*] **, Hiroki Kondo** [2] **, Mineo Hiramatsu** [1] **and Masaru Hori** [2]

1 Department of Electrical and Electronic Engineering, Meijo University, 1-501 Shiogamaguchi, Tempaku, Nagoya 468-8502, Japan
2 Center of Low Temperature Plasma Sciences, Nagoya University, Nagoya 464-8601, Japan
* Correspondence: ishikawa.kenji@nagoya-u.jp; Tel.: +81-52-789-6077

Abstract: Carbon nanowalls (CNWs), vertically standing highly crystallizing graphene sheets, were used in the application of a surface-assisted laser desorption/ionization time-of-flight mass spectrometry (SALDI-TOF-MS). The CNW substrates solved the issues on interferences of matrix molecules and alkali metal addition ions in low-weight molecule detection. Before SALDI sample preparations, the hydrophobic CNW was treated by atmospheric pressure plasma for exposing hydrophilicity to the CNWs' surface. Detection of water soluble amino acids, arginine, was demonstrated.

---

1. Introduction

For rapid, invasive, and sensitive sampling of biological fluids, matrix-assisted laser desorption/ionization (MALDI) mass spectrometry (MS) analyses have attracted great interests, owing to soft ionization properties of biomolecules, such as proteins and amino acids. However, MALDI mass spectra are convolved with peaks of matrix-related fragments and alkali metal cation adducts in the low-molecular-weight region, or possibly for low-molecular-weight analytes less than 700 in a mass-to-charge ratio (m/z) [1].

To solve these drawbacks, matrix-free, surface-assisted laser desorption/ionization mass spectrometry (SALDI-MS) is a matrix-free photo-desorption/ionization method, first reported in 1995 by Sunner et al. [2] and reviewed elsewhere [3–6]. Inorganic nanoparticles or nanostructured surfaces (nanostructures or nanoparticles of platinum [7–11], titanium or titania [12–17], iron oxides [18,19], silver [20], silicon [21,22], etc.) were reported to use them as SALDI substrates [23–28]. Furthermore, alkali metal addition ions such as $[M+K]^+$ or $[M+Na]^+$ of biomolecules (M) were sometimes introduced to ionization processes and suppressed mass spectrometric signals. Very recently, for this, the use of carbon nanomaterials (graphite, graphene, carbon nanotubes, carbon black, and polymeric nanofibers) as SALDI substrates has been rapidly growing in SALDI applications [29–46]. These carbon forms are different in an optical absorption property. In the view of the matrix property, graphite is a candidate for utilization in the SALDI process. However, sample preparation with carbon nanomaterials as SALDI substrates is relatively complex.

Carbon nanowalls (CNWs) are a nanostructured carbon material that stands vertically on the substrate and are grown starting with a collection of graphene sheets using various chemical vapor

deposition (CVD) methods [47,48]. The graphene sheets form a self-supported network of wall structures with thicknesses ranging from a few nanometers to a few tens of nanometers. CNWs have a high density of graphene edges at an atomic scale. These characteristics have the potential to enhance laser desorption/ionization. The electric fields formed by the laser irradiation are strengthened not only by strong localization at the edges of the wall structure of the CNWs but also because the graphitic property of the CNWs effectively absorbs the energy of the photons, thus serving as an energy transfer medium onto the analytes. Indeed, hydrophobic and boron-doped CNWs for SALDI-MS of small compounds, such as glucose, melamine, dopamine, and acetaminophen, providing a detection of metabolites as a matrix-free LDI method were reported [49]. Very recently, in comparison with matrix molecules, pure carbon materials are considered to be superior for easy cleaning of the ion source after LDI analysis. Therefore, the matrix-free LDI procedure has been optimized by controlling a surface property of CNWs by the atmospheric pressure plasma treatments.

In this study, the CNWs SALDI-MS were investigated in detail. An atmospheric pressure plasma treatment was tried, aiming for modification of the CNWs' surface. LDI efficiency of arginine was investigated, because amino acids are generally difficult to ionize; however, the ion yield of arginine in positive ion mode was relatively high among amino acids.

2. Materials and Methods

2.1. CNWs Substrate

CNWs films were synthesized on the silicon substrate with plasma-enhanced chemical vapor deposition (CVD) by using the inductively coupled plasma source. Details are described elsewhere [47,48]. The radio frequency (RF) power was 550 W; Ar/CH_4 gas flow rates were 20/50 sccm; total pressure was 3.07 Pa; growth temperature was 720 °C; and growth time was one hour. Figure 1 shows (a) plane-view and (b) cross-sectional-view scanning electron microscopy (SEM) images of CNWs. The height of the CNW was 1.5 μm. The wall density was calculated to be 24 (unit/μm^2), which is defined by the number of walls per unit length, from the plane view [50].
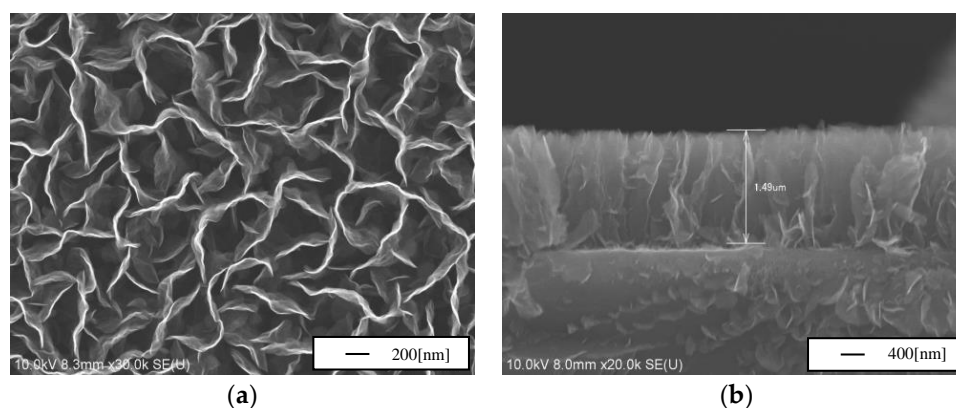

Figure 1. Scanning electron microscopy (SEM) image of carbon nanowall (CNW) on Si substrate; (**a**) plane view, (**b**) cross-sectional view.

Figure 2 shows Raman spectra of CNWs. Peaks regarding typical CNWs are observed at around 1350 cm^{-1} for D band (disordered induced peak), 1580 cm^{-1} for G band (graphite peak), 1620 cm^{-1} for D' band (symmetry breaking due to finite sp^2 crystalline size), 2700 cm^{-1} for 2D(G') band (second order of the D peak), and 2950 cm cm^{-1} for D+G (D'') band (combination band of D and G peaks).
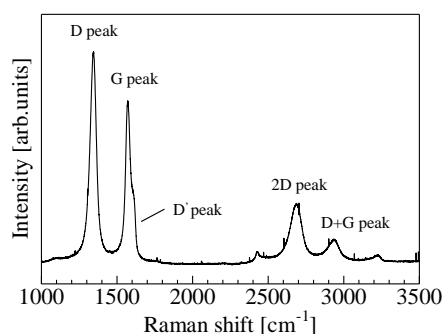
Figure 2. Raman spectra of CNWs.

2.2. Arginine Sample Preparation

The sample was arginine ($C_6H_{14}N_4O_2$; 174 amu). Purified L-arginine hydrochloride (Sigma-Aldrich A5131, Merck KGaA Japan) was dissolved in ultrapure water (Milli-Q). The concentration was adjusted to be 50 mM. Then, 5 µL of the aqueous solution was dropped on the CNWs/Si substrate and dried under ambient air.

2.3. SALDI Setup

Figure 3 shows the schematic diagram of a time-of-flight mass spectrometer (TOF-MS; Toyama, Japan). Background pressures of the ionization chamber and the TOF chamber were kept below 10^{-7} Pa. The sample was placed in the ionization chamber. The sample surface on the CNW/Si substrate was irradiated with a fourth harmonic with a wavelength of 266 nm of a Nd: YAG laser (repetition rate: 30 Hz; pulse width: 2 ns; Spectra-Physics Quanta-Ray Pro 250). By triggering the laser shots, desorption/ionization of the sample occurred and the ions were collected by the electrostatic lens of an extractor electrode and transported to the TOF chamber. The reflectron realized a high resolution measurement of the flight time. The ion signal was detected with a micro-channel plate (MCP) in the positive ion mode with application of a high voltage of 2 kV.
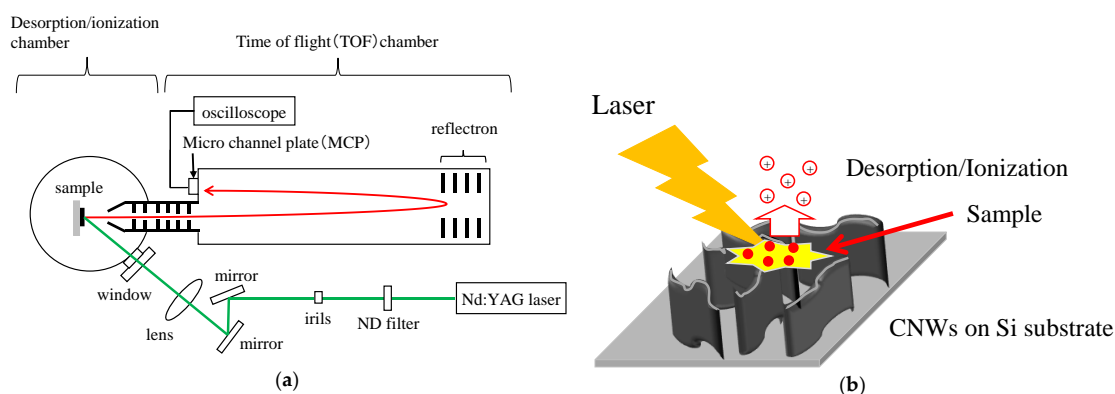

Figure 3. Schematic diagram of (**a**) surface-assisted laser desorption/ionization time-of-flight mass spectrometry (SALDI-TOF-MS) system; (**b**) illustration of desorption/ionization process on CNWs.

2.4. Surface Characterization

After the CVD growth of the CNWs, the CNWs exhibited hydrophobic properties. The hydrophilic surface of the CNWs was formed by treatment using atmospheric pressure plasma [51]. A high voltage of 6 kV was applied; Ar gas flow rate was 1.5 slm; irradiation time was 30 s; and the distance from the plasma to the CNWs/Si substrate was 5 mm.

After dropping and drying the arginine-containing solution on the CNWs/Si substrate, samples were observed by SEM (SU-8200, Hitachi-High Technologies, Japan).

3. Results and Discussion

CNWs-SALDI-MS

First, two samples were prepared by (a) without or (b) with atmospheric pressure plasma treatment of the CNWs/Si substrate. Then, the arginine-dissolved solution was dropped on it. Figure 4 shows SEM images of boundary regions between the arginine-containing solution-dropped areas and the bare CNW surface. The arginine dropped areas are observed by darkness in brightness and smooth morphology. On the plasma-treated CNW surface, the droplet tended to spread widely over the surface. The hydrophilic property was observed by macroscopic water contact angle measurements. Figure 5 shows contact angle images for droplets of water on the CNWs/Si substrate, (a) without or (b) with hydrophilic treatment of the CNWs. Depending on the surface characteristics, distribution of the deposited arginine became wider for the hydrophilic surface than that of the initial hydrophobic surface.
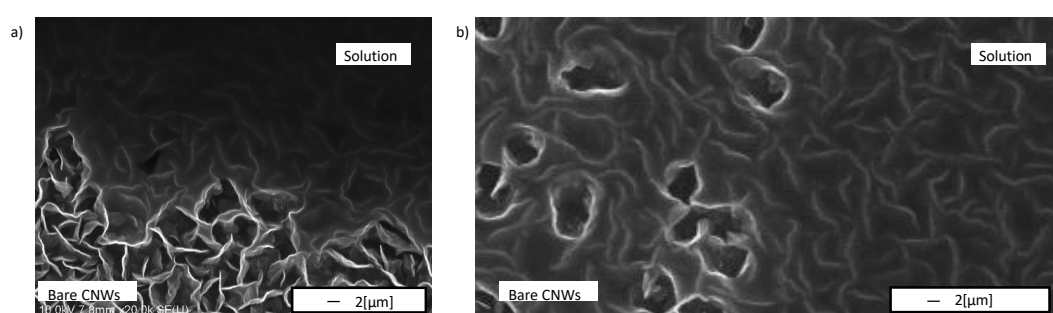

Figure 4. SEM images of the CNWs/Si substrate, after dropping the arginine-dissolved solution on the CNW surface, treated (**a**) without or (**b**) with atmospheric pressure plasma.
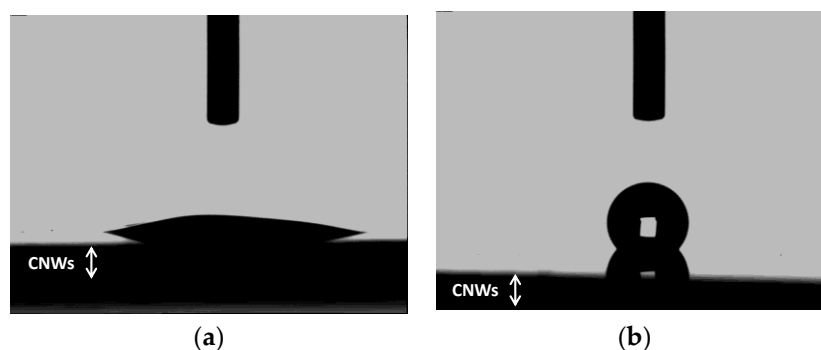

Figure 5. Contact angle images for droplets of water on the CNWs/Si substrate, (**a**) without or (**b**) with atmospheric pressure plasma treatment of the CNWs.

The hydrophilicity was introduced to the as-deposited hydrophobic CNWs films. The treatments using atmospheric pressure plasma were carried out with air entrainment. The entrained oxygen molecules were dissociated and highly reactive oxygen atoms reacted with the CNW surface with the formation of hydroxyl groups, carboxyl group, and carbonyl groups. A similar report was found elsewhere [52].

Figure 6 shows SALDI mass spectra of the sample coated on the hydrophobic CNW substrate as a surface-assisted material. The measurement conditions were fixed with a laser energy of 0.6 mJ. Without the arginine on the CNW/Si substrate as shown in Figure 6a, the signals from sodium and potassium were observed at m/z of 23 and 39, respectively. These signals originated from saline. If samples dissolve in saline solution, these signals are observable in a mass spectrum. The other mass signals were originated from the hydrophobic CNWs/Si substrate. The signals were observed at m/z of 108, 120, 132, 144, 156, 168, and 180, originating from CNWs, as shown in Figure 6c.
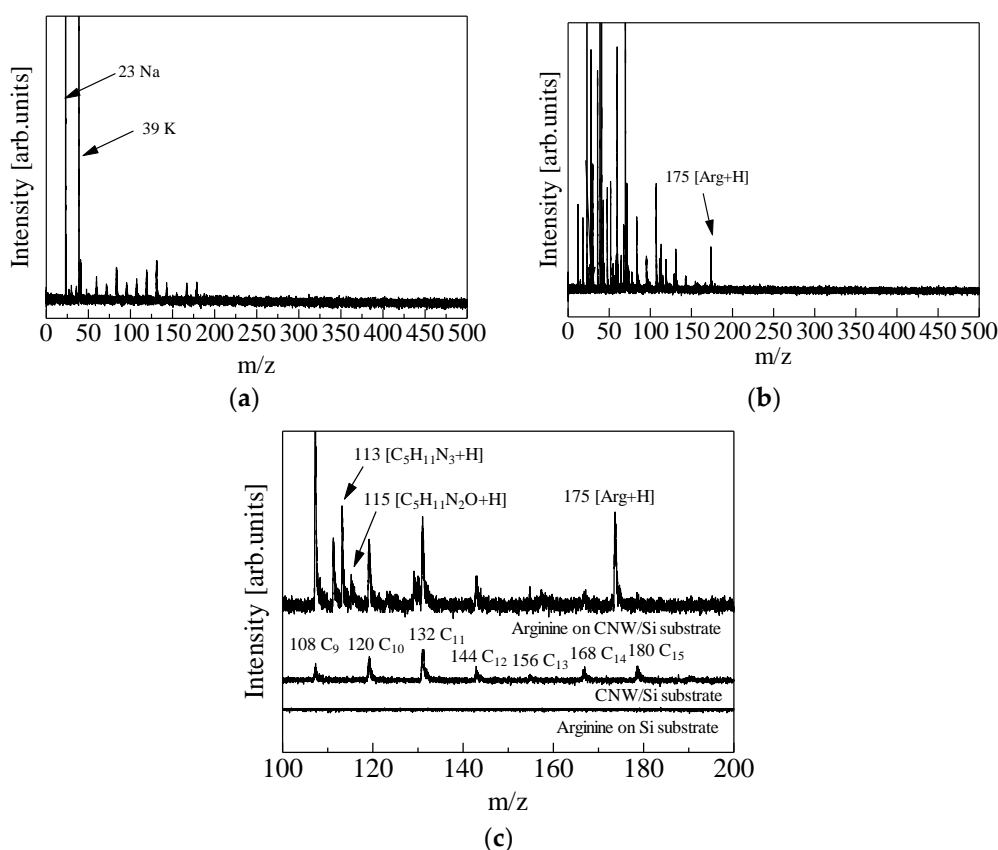
Figure 6. SALDI mass spectra. (**a**) CNW/Si substrate from 0 to 500 in m/z, (**b**) arginine on CNW/Si substrate from 0 to 500 in m/z, (**c**) enlargement from 100 to 200 in m/z, arginine on CNW/Si substrate, no sample on CNW/Si substrate, and arginine on Si substrate.

As shown in Figure 6b, with the arginine sample on CNW/Si substrate, a signal at m/z of 175 is clearly observed. This signal can be identified as the protonated ion of arginine (Arg+H) [53]. In addition, the signals from carbon and silicon were observed at m/z of 12 and 28, as well as sodium and potassium. Figure 6c shows the enlargement of SALDI mass spectra from 100 to 200 in m/z, arginine on CNW/Si substrate, no sample on CNW/Si substrate, and arginine on Si substrate. The signals of fragments of arginine were observed at m/z of 113 and 115, as well as the signal at m/z of 175, which were assigned to ($C_5H_{11}N_3$+H) and ($C_5H_{11}N_2O$+H), respectively (Figure 6c). Clearly, the LDI effect was achieved by using the CNW substrate as a surface-assisted material in comparison with arginine on Si substrate.

Next, the dependence of surface characteristic of the CNWs films was studied. Figure 7 shows SALDI mass spectra of arginine on CNWs with and without the atmospheric pressure plasma treatment. The signal intensity was normalized by dividing the signal intensity of the silicon substrate at m/z 28. The normalized signal intensity of arginine and the signal-to-noise ratio are summarized in Table 1. In this case, the arginine signal on the hydrophilic CNWs was larger than that on the CNWs without the atmospheric pressure treatment. In addition, the signal at m/z of 159, originating from the protonated ion of ($C_6H_{12}N_3O_3$+H), could be detected. This fragment was produced by desorption of NH_2 (m/z 16) from the arginine, due to the laser irradiation [54]. The normalized intensity of arginine showed a maximum at optimal laser energy, because the laser energy was effectively transferred to the LDI of arginine. In the ionization process of the laser pulse, the proton transfer is supported by charge separation and their relaxation time of these charges. The latter relaxation strongly depends on the nature of the substrate. In [55], the silicon substrate, as a semiconductor, possesses a band gap and extends the relaxation. In the case of graphitic carbons, the charge recombination time is expected to be much faster, thus hindering the reaction of proton transfer from OH groups to the analyte. Possibly, the

laser-pulse induces the direct dissociative ionization process of the analyte. Accordingly, an optimal laser power exists; in this case, the highest signal-to-noise ratio was obtained at 0.23 mJ. The conditions for the atmospheric pressure plasma treatment and the laser energy should be further optimized to avoid fragmentation that induces background interference for each analyte.
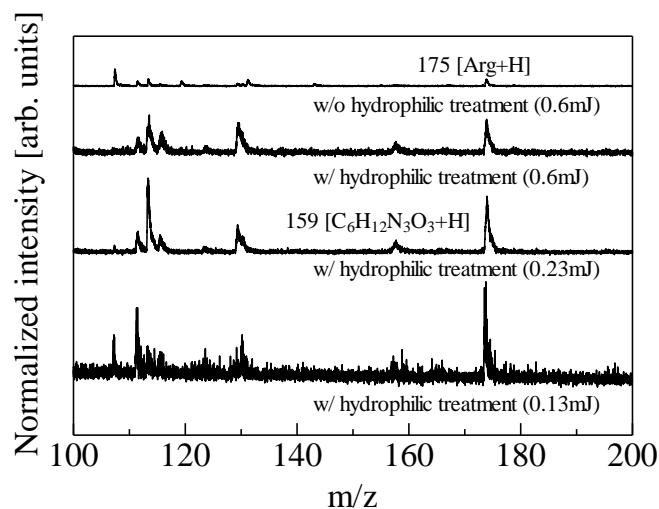

Figure 7. Mass spectra of arginine with and without hydrophilic treatment.

Table 1. Normalized signal intensity of arginine and signal-to-noise (S/N) ratios.

Atmospheric Pressure Plasma Treatment	Laser Energy	Normalized Intensity of Arginine	S/N Ratio
Without	0.60	0.18	9.0
With	0.60	0.87	6.7
	0.23	1.60	17.8
	0.13	2.80	10.1

The surface treatments of the CNW films are easily conducted by the atmospheric pressure plasma. As demonstrated in this study, water-soluble arginine solution was well dispersed on the hydrophilic CNWs surface. A major point might be found in drying of the solution. If the water droplet drops on a hydrophobic surface, evaporation or drying of the dropped areas forms a boundary of a gas–liquid–solid interface. Water-soluble species on the initial surface can dissolve in the droplet and particles can float on the droplet. Unfortunately, these contaminants may be concentrated at the interface boundary after the evaporation. According to this, well-spread distribution of analytes on the hydrophilic surface plays a key role for increasing LDI intensity at the optimal condition. In essence, the CNW-SALDI-MS with a 266-nm laser light was operated with laser-induced direct dissociative ionization with proton transfer. Therefore, the surface treatments of the CNW substrates are a useful way of improving efficiency and sensitivity of desorption/ionization of analytes.

4. Conclusions

The CNWs-SALDI-MS was demonstrated for a matrix-free LDI-MS by detection of arginine in positive ion mode. When the CNWs substrate was treated by the atmospheric pressure plasma, the hydrophilic surface of CNWs was exposed. In the case of water-soluble samples, the hydrophilic CNWs improved in sensitivity of the SALDI-MS measurements. Using a 266-nm-wavelength laser light, the ionization process of analytes mainly occurred by direct dissociate ionization with proton transfer. The highest signal-to-noise ratio depended on the laser energy; in this case, an optimal energy appeared at 0.23 mJ. The surface treatments and CNWs are useful for the LDI-MS methods.

References

1. Karas, M.; Kruger, R. Ion formation in MALDI: The cluster ionization mechanism. *Chem. Rev.* **2002**, *103*, 427–440. [CrossRef] [PubMed]

2. Sunner, J.; Dratz, E.; Chen, Y.-C. Graphite surface-assisted laser desorption/ionization time-of-flight mass spectrometry of peptides and proteins from liquid solutions. *Anal. Chem.* **1995**, *67*, 4335–4342. [CrossRef] [PubMed]

3. Peterson, D.S. Marix-free methods for laser desorption/ionization mass spectrometry. *Mass Spectrom. Rev.* **2007**, *26*, 19–34. [CrossRef] [PubMed]

4. Arakawa, R.; Kawasaki, H. Functionalized nanoparticles and nanostructured surfaces for surface-assisted laser desorption/ionization mass spectrometry. *Anal. Sci.* **2010**, *26*, 1229–1240. [CrossRef] [PubMed]

5. Chiang, C.-K.; Chen, W.-T.; Chang, H.-T. Nanoparticle-based mass spectrometry for the analysis of biomolecules. *Anal. Chem. Soc. Rev.* **2011**, *40*, 1269–1281. [CrossRef] [PubMed]

6. Law, K.P.; Larkin, J.R. Recent advances in SALDI-MS techniques and their chemical and bioanalytical applications. *Anal. Bioanal. Chem.* **2011**, *399*, 2597–2622. [CrossRef] [PubMed]

7. Kawasaki, H.; Yonezawa, T.; Watanabe, T.; Arakawa, R. Platinum nanoflowers for surface-assisted laser desorption/ionization mass spectrometry of biomolecules. *J. Phys. Chem. C* **2007**, *111*, 16278–16283. [CrossRef]

8. Yonezawa, T.; Kawasaki, H.; Tarui, A.; Watanabe, T.; Arakawa, R.; Shimada, T.; Mafune, F. Detailed investigation on the possibility of nanoparticles of carious metal elements for surface-assisted laser desorption/ionization mass spectrometry. *Anal. Sci.* **2009**, *25*, 339. [CrossRef]

9. Kawasaki, H.; Yao, T.; Suganuma, T.; Okumura, K.; Iwaki, Y.; Yonezawa, T.; Kikuchi, T.; Arakawa, R. Platinum nanoflowers on scratched silicon by galvanic displacement for an effective SALDI substrate. *Chem. Eur. J.* **2010**, *16*, 10832–10843. [CrossRef]

10. Yao, T.; Kawasaki, H.; Watanabe, T.; Arakawa, R. Effectiveness of platinum particle deposition on silicon surfaces for surface-assisted laser desorption/ionization mass spectrometry of peptides. *Int. J. Mass Spectrom.* **2010**, *291*, 145–151. [CrossRef]

11. Nitta, S.; Kawasaki, H.; Suganuma, T.; Shigeri, Y.; Arakawa, R. Desorption/ionization efficiency of common amino acids in surface-assisted laser desorption/ionization mass spectrometry (SALDI-MS) with Nanostructured Platinum. *J. Phys. Chem. C* **2013**, *117*, 238–245. [CrossRef]

12. Lo, C.-Y.; Lin, J.-Y.; Chen, W.-Y.; Chen, C.-T.; Chen, Y.-C. Surface-assisted laser desorption/ionization mass spectrometry on titania nanotube arrays. *J. Am. Soc. Mass Spectrom.* **2008**, *19*, 1014–1020. [CrossRef] [PubMed]

13. Kawasaki, H.; Okumura, K.; Arakawa, R. Influence of crystalline forms of titania on desorption/ionization efficiency in titania-based surface-assisted laser desorption/ionization mass spectrometry. *J. Mass Spectrom. Soc. Jpn.* **2010**, *58*, 221–228. [CrossRef]

14. Sonderegger, H.; Rameshan, C.; Lorenz, H.; Klauser, F.; Klerks, M.; Rainer, M.; Bakry, R.; Huck, C.W.; Bonn, G.K. Surface-assisted laser desorption/ionization-mass spectrometry using TiO$_2$-coated steel targets for the analysis of small molecules. *Anal. Bioanal. Chem.* **2011**, *401*, 1963. [CrossRef] [PubMed]

15. Osaka, I.; Okumura, K.; Miyake, N.; Watanabe, T.; Nozaki, K.; Kawasaki, H.; Arakawa, R. Quantitative analysis of an antioxidant additive in insoluble plastics by surface-assisted laser desorption/ionization mass spectrometry (SALDI-MS) using TiO$_2$ nanoparticles. *J. Mass Spectrom. Soc. Jpn.* **2010**, *58*, 123–127. [CrossRef]

16.   Popovic, I.; Nesic, M.; Vranjes, M.; Saponjic, Z.; Petkovic, M. TiO$_2$ nanocrystals–assisted laser desorption and ionization time-of-flight mass spectrometric analysis of steroid hormones, amino acids and saccharides. Validation and comparison of methods. *RSC Adv.* **2016**, *6*, 1027–1036. [CrossRef]

17.   Gao, C.; Zhen, D.; He, N.; An, Z.; Zhou, Q.; Li, C.; Grimes, C.A.; Cai, Q. Two-dimensional TiO$_2$ nanoflakes enable rapid SALDI-TOF-MS detection of toxic small molecules (dyes and their metabolites) in complex environments. *Talanta* **2019**, *196*, 1–8. [CrossRef] [PubMed]

18.   Iwaki, Y.; Kawasaki, H.; Arakawa, R. Human serum albumin-modified Fe$_3$O$_4$ magnetic nanoparticles for affinity-SALDI-MS of small-molecule drugs in biological liquids. *Anal. Sci.* **2012**, *28*, 893–900. [CrossRef]

19.   Kusano, M.; Kawabata, S.; Tamura, Y.; Mizoguchi, D.; Murouchi, M.; Kawasaki, H.; Arakawa, R.; Tanaka, K. Laser desorption/ionization mass spectrometry (LDI-MS) of lipids with iron oxide nanoparticle-coated targets. *Mass Spectrom.* **2014**, *3*, A0026. [CrossRef] [PubMed]

20.   Zhu, Q.; Teng, F.; Wang, Z.; Wang, Y.; Lu, N. Superhydrophobic glass substrates coated with fluorosilane-coated silica nanoparticles and silver nanoparticles for surface-assisted laser desorption/ionization mass spectrometry. *ACS Appl. Nano Mater.* **2019**, *2*, 3813–3818. [CrossRef]

21.   Go, E.P.; Prenni, J.E.; Wei, J.; Jones, A.; Hall, S.C.; Witkowska, H.E.; Shen, Z.; Siuzdak, G. Desorption/ionization on silicon time-of-flight/time-of-flight mass spectrometry. *Anal. Chem.* **2003**, *75*, 2504–2506. [CrossRef] [PubMed]

22.   Korte, A.R.; Stopka, S.A.; Morris, N.; Razunguzwa, T.; Vertes, A. Large-scale metabolite analysis of standards and human serum by laser desorption ionization mass spectrometry from silicon nanopost arrays. *Anal. Chem.* **2016**, *388*, 8989–8996. [CrossRef] [PubMed]

23.   Aminlashgari, N.; Hakkarainen, M. Surface assisted laser desorption ionization-mass spectrometry (SALDI-MS) for analysis of polyester degradation products. *J. Am. Soc. Mass Spectrom.* **2012**, *23*, 1071–1076. [CrossRef] [PubMed]

24.   Lim, A.Y.; Ma, J.; Boey, Y.C.F. Development of nanomaterials for SALDI-MS analysis in forensics. *Adv. Mater.* **2012**, *24*, 4211–4216. [CrossRef] [PubMed]

25.   Chen, W.-T.; Chiang, C.-K.; Lee, C.-H.; Chang, H.-T. Using surface-assisted laser desorption/ionization mass spectrometry to detect proteins and protein−protein complexes. *Anal. Chem.* **2012**, *84*, 1924–1930. [CrossRef] [PubMed]

26.   Chen, W.-T.; Chang, H.-T. Tea identification through surface-assisted laser desorption/ionization mass spectrometry. *Int. J. Anal. Mass Spectrom. Chromatogr.* **2013**, *1*, 11. [CrossRef]

27.   Fujita, T.; Shibamoto, K. Surface-assisted laser desorption-ionization mass spectrometry of oligosaccharides. *Chem. Lett.* **2013**, *42*, 852. [CrossRef]

28.   Grechnikov, A.A. Analytical capabilities of surface-assisted laser desorption/ionization in the determination of low-molecular-weight volatile compounds. *J. Anal. Chem.* **2015**, *70*, 1047–1054. [CrossRef]

29.   Amini, N.; Shariatgorji, M.; Thorsén, G. SALDI-MS signal enhancement using oxidized graphitized carbon black nanoparticles. *J. Am. Soc. Mass Spectrom.* **2009**, *20*, 1207–1213. [CrossRef]

30.   Kim, Y.-K.; Na, H.-K.; Kwack, S.-J.; Ryoo, S.-R.; Lee, Y.; Hong, S.; Hong, S.; Jeong, Y.; Min, D.-H. Synergistic effect of graphene oxide/MWCNT films in laser desorption/ionization mass spectrometry of small molecules and tissue imaging. *ACS Nano* **2011**, *5*, 4550–4561. [CrossRef]

31.   Zhang, J.Y.; Li, Z.; Zhang, C.; Feng, B.; Zhou, Z.; Bai, Y.; Liu, H. Graphite-coated paper as substrate for high sensitivity analysis in ambient surface-assisted laser desorption/ionization mass spectrometry. *Anal. Chem.* **2012**, *84*, 3296–3301. [CrossRef] [PubMed]

32.   Liu, C.-W.; Chien, M.-W.; Su, C.-Y.; Chen, H.-Y.; Li, L.-J.; Lai, C.-C. Analysis of flavonoids by graphene-based surface-assisted laser desorption/ionization time-of-flight mass spectrometry. *Analyst* **2012**, *137*, 5809–5816. [CrossRef] [PubMed]

33.   Lu, T.; Olesik, V. Electrospun nanofibers as substrates for surface-assisted laser desorption/ionization and matrix-enhanced surface-assisted laser desorption/ionization mass spectrometry. *Anal. Chem.* **2013**, *85*, 4384–4391. [CrossRef] [PubMed]

34.   Ma, R.; Lu, M.; Ding, L.; Ju, H.; Cai, Z. Surface-assisted laser desorption/ionization mass spectrometric detection of biomolecules by using functional single-walled carbon nanohorns as the matrix. *Chem. Eur. J.* **2013**, *19*, 102–108. [CrossRef] [PubMed]

35. Kim, Y.-K.; Min, D.-H. Mechanistic study of laser desorption/ionization of small molecules on graphene oxide multilayer films. *Langmuir* **2014**, *30*, 12675–12683. [CrossRef] [PubMed]

36. Shih, Y.-H.; Fu, C.-P.; Liu, W.-L.; Lin, C.-H.; Huang, H.-Y.; Ma, S. Nanoporous carbons derived from metal-organic frameworks as novel matrices for surface-assisted laser desorption/ionization mass spectrometry. *Small* **2016**, *12*, 2057–2066. [CrossRef] [PubMed]

37. Kosyakov, D.S.; Sorokina, E.A.; Ul'yanovskii, N.V.; Varakin, E.A.; Chukhchin, D.G.; Gorbova, N.S. Carbon nanocoatings: A new approach to recording mass spectra of low-molecular compounds using surface-assisted laser desorption/ionization mass spectrometry. *J. Anal. Chem.* **2016**, *71*, 1221–1227. [CrossRef]

38. Wang, J.; Liu, Q.; Liang, Y.; Jiang, G. Recent progress in application of carbon nanomaterials in laser desorption/ionization mass spectrometry. *Anal. Bioanal. Chem.* **2016**, *408*, 2861–2873. [CrossRef]

39. Bian, J.; Olesik, S.V. Surface-assisted laser desorption/ionization time-of-flight mass spectrometry of small drug molecules and high molecular weight synthetic/biological polymers using electrospun composite nanofibers. *Analyst* **2017**, *142*, 1125–1132. [CrossRef]

40. Li, X.; Xu, G.; Zhang, H.; Liu, S.; Niu, H.; Peng, J.; Wu, J.; Wu, R. A homogeneous carbon nanosphere film-spot: For highly efficient laser desorption/ionization of small biomolecules. *Carbon* **2017**, *121*, 343–352. [CrossRef]

41. Feng, D.; Xia, Y. Covalent organic framework as efficient desorption/ionization matrix for direct detection of small molecules by laser desorption/ionization mass spectrometry. *Anal. Chim. Acta* **2018**, *1014*, 58–63. [CrossRef]

42. Lu, W.; Li, R.; Shuang, S.; Dong, C.; Cai, Z. Reduced carbon nanodots as a novel substrate for direct analysis of bisphenol analogs in surface assisted laser desorption/ionization time of flight mass spectrometry. *Talanta* **2018**, *190*, 89–94. [CrossRef] [PubMed]

43. Teng, F.; Zhu, Q.; Wang, Y.; Du, J.; Lu, N. Enhancing reproducibility of SALDI MS detection by concentrating analytes within laser spot. *Talanta* **2018**, *179*, 583–587. [CrossRef]

44. Wang, S.; Niu, H.; Cao, D.; Cai, Y. Covalent-organic frameworks as adsorbent and matrix of SALDI-TOF MS for the enrichment and rapid determination of fluorochemicals. *Talanta* **2019**, *194*, 522–527. [CrossRef] [PubMed]

45. Coffinier, Y.; Boukherroub, R.; Szunerits, S. Carbon-based nanostructures for matrix-free mass spectrometry. In *Carbon Nanoparticles and Nanostructures*; Yang, N., Jiang, X., Pang, D.W., Eds.; Springer: Berlin, Germany, 2016; pp. 331–356. [CrossRef]

46. Hosu, I.S.; Sobaszek, M.; Ficek, M.; Bogdanowicz, R.; Drobecq, H.; Boussekey, L.; Barras, A.; Melnyk, O.; Boukherrouba, R.; Coffinier, Y. Carbon nanowalls: A new versatile graphene based interface for the laser desorption/ionization-mass spectrometry detection of small compounds in real samples. *Nanoscale* **2017**, *9*, 9701–9715. [CrossRef] [PubMed]

47. Hiramatsu, M.; Hori, M. *Carbon Nanowalls*; Springer: Berlin, Germany, 2010. [CrossRef]

48. Hiramatsu, M.; Kondo, H.; Hori, M. Graphene Nanowalls. In *New Progress on Graphene Research*; BoD–Books on Demand: Norderstedt, Germany, 2013; pp. 235–260. [CrossRef]

49. Chen, Y.; Chen, H.; Aleksandrov, A.; Orlando, T.M. Roles of water, acidity, and surface morphology in surface-assisted laser desorption/ionization of amino acids. *J. Phys. Chem. C* **2008**, *112*, 6953–6960. [CrossRef]

50. Cho, H.J.; Kondo, H.; Ishikawa, K.; Sekine, M.; Hiramatsu, H.; Hori, M. Density control of carbon nanowalls grown by CH_4/H_2 plasma and their electrical properties. *Carbon* **2014**, *68*, 380–388. [CrossRef]

51. Iwasaki, M.; Inui, H.; Matsudaira, Y.; Kano, H.; Yoshida, N.; Ito, M.; Hori, M. E Nonequilibrium atmospheric pressure plasma with ultrahigh electron density and high performance for glass surface cleaning. *Appl. Phys. Lett.* **2008**, *92*, 081503. [CrossRef]

52. Watanabe, H.; Kondo, H.; Sekine, M.; Hiramatsu, M.; Hori, M. Control of super hydrophobic and super hydrophilic surfaces of carbon nanowalls using atmospheric pressure plasma treatments. *Jpn. J. Appl. Phys.* **2012**, *51*, 01AJ07. [CrossRef]

53. Beuhler, R.J.; Flanigan, E.; Greene, L.J.; Friedman, L. Proton transfer mass spectrometry of peptides a rapid heating technique for underivatized peptides containing arginine. *J. Am. Chem. Soc.* **1974**, *12*, 3990–3999. [CrossRef]

54. Forbes, M.W.; Jockusch, R.A.; Young, A.B.; Harrison, A.G. Fragmentation of protonated dipeptides containing arginine. Effect of activation method. *J. Am. Soc. Mass Spectrom.* **2007**, *18*, 1959–1966. [CrossRef] [PubMed]

55. Alimpiev, S.; Grechnikov, A.; Sunner, J.; Karavansky, V.; Simanovsky, Y.; Zhabin, S.; Nikiforov, S. On the role of defects and surface chemisrty for surface-assisted laser desorption ionization from silicon. *J. Chem. Phys.* **2008**, *128*, 014711. [CrossRef] [PubMed]